

## Rapid Communications

The Rapid Communications section is intended for the accelerated publication of important new results. Since manuscripts submitted to this section are given priority treatment both in the editorial office and in production, authors should explain in their submittal letter why the work justifies this special handling. A Rapid Communication should be no longer than 3½ printed pages and must be accompanied by an abstract. Page proofs are sent to authors, but, because of the accelerated schedule, publication is not delayed for receipt of corrections unless requested by the author or noted by the editor.

### Dynamic modes of one-dimensional Josephson tunnel junctions

S. Meepagala, J. T. Chen, and Jhy-Jiun Chang

Department of Physics and Astronomy, Wayne State University, Detroit, Michigan 48202

(Received 20 March 1987)

A study that combines experimental measurements of the effects of a focused laser beam on the current-voltage characteristics and computer simulations of Josephson tunnel junctions shows that there are different dynamic modes which are responsible for the zero-field current steps at finite voltages. One of the modes is associated with the soliton-antisoliton propagation. The dc tunneling current in this case is found to be predominantly the zero-voltage pair current flowing near the junction edges. The other mode can be attributed to the standing-wave excitations of electromagnetic waves. The dc tunneling current of this mode is spatially oscillatory.

The dynamic modes of a one-dimensional Josephson tunnel junction were often investigated by using a modified sine-Gordon equation that governs the phase-difference function  $\phi(x, t)$  of the junction:<sup>1</sup>

$$\left( \frac{\partial^2}{\partial x^2} - \frac{\partial^2}{\partial t^2} - \gamma \frac{\partial}{\partial t} \right) \phi(x, t) = \sin \phi(x, t) + \eta(x), \quad (1)$$

with the boundary conditions

$$\left. \frac{\partial \phi(x, t)}{\partial x} \right|_L = H_a + I, \quad \left. \frac{\partial \phi(x, t)}{\partial x} \right|_0 = H_a - I, \quad (2)$$

where the distance  $x$  and the time  $t$  are in units of the Josephson penetration depth  $\lambda_J$  and the inverse of the plasma angular frequency  $\omega_J = c/\lambda_J$ , respectively, and  $c$  is the speed of the electromagnetic waves in the junction. There is a variety of solutions depending on the boundary conditions, the distribution of the bias current  $\eta$ , the ratio of the junction length and the Josephson penetration depth, and the loss parameter  $\gamma$ . One well-known solution corresponds to the propagation of a soliton-antisoliton.<sup>2</sup> Experimentally, this dynamic mode can be observed as an Ohmiclike current step in the current-voltage ( $I$ - $V$ ) characteristics.<sup>3</sup> Similar current steps at nearly constant voltages have also been observed in shorter junctions and were attributed to the excitation of electromagnetic cavity modes.<sup>4,5</sup> Experimentally, there are some difficulties in identifying the detailed nature of the dynamic modes using  $I$ - $V$  characteristic measurements alone. Because  $I$ - $V$  curves show only the space- and time-averaged current and voltage, they are not very sensitive to different mechanisms. Moreover, even if the mechanism has been identified, further studies are required to probe the de-

tailed nature of the mode, such as the spatial distribution of the dc tunneling current. In the past, we have used the scanning focused-laser-beam technique<sup>6</sup> to investigate the current distribution in Josephson junctions biased at zero voltage, where the junctions are in the static state. In this article, we demonstrate that the same technique can be used to study the dynamic states.<sup>7</sup> Our experimental results along with those from computer simulations reveal in a direct manner that there are at least two fundamentally different modes which can be responsible for the zero-field current steps. Furthermore, the data also show clearly that for junctions in a soliton-antisoliton mode, the dc current is mainly contributed by the pair current flowing through the edges. However, for junctions with standing-wave excitations, the dc current has a spatially oscillatory distribution.

The principle of the experimental technique is as follows. A weak laser beam is focused on a small area of the junction to serve as a weak heat source which weakens the superconductivity locally. The change in the maximum current of the step is then measured as the laser is scanned across the junction. In the zero-voltage case, the junction is in the static state, the change in the maximum current as a function of the laser position was found to reflect the pair-current distribution in the junction.<sup>6</sup> This is especially true at an applied field where current has a local maximum value. For other fields, nonlocal effects may change the spatial dependence of the current density.<sup>8</sup> In the finite-voltage case the junction is in a dynamic state, and the quasiparticle current will play a role. We found that this technique can also reveal information about the current distributions. The spatial dependences of the laser irradiation on the maximum zero-voltage current as well

as the first two steps are shown in Figs. 1(a)–1(c).

The samples are Pb/PbO/Pb tunnel junctions prepared by conventional evaporation and oxidation technique. They are of overlap geometry. The dimension of the first one is  $0.86 \times 0.11 \text{ mm}^2$ . The  $I$ - $V$  characteristic has four zero-field current steps with a maximum zero-voltage current  $I_0 = 35.5 \text{ mA}$  at 4.2 K when no magnetic field is applied.  $I_0$  can be increased to 38 mA by applying a magnetic field of 0.35 G to compensate the self-field due to the built-in asymmetry of the junction. The junction resistance in the normal state is  $0.015 \text{ } \Omega$ , giving a Josephson current density  $j_0 = 130 \text{ A/cm}^2$ . This value of  $j_0$ , together with the London penetration depth  $\lambda_J = 50 \text{ nm}$ , yields a ratio  $L/2\pi\lambda_J = 3$ . Thus this junction can be classified as a long junction capable of accommodating a soliton which has a typical size of  $2\pi\lambda_J$ . In all the data shown, the laser intensity was kept below  $100 \text{ } \mu\text{W}$  over a circular area of radius  $15 \text{ } \mu\text{m}$ , where the measured structure was found to be independent of the power level.

Figures 1(a)–1(c) show that the spatial dependences of the changes in  $I_0$ ,  $I_1$ , and  $I_2$  are all similar, indicating that in the dynamic state the junction current also mainly flows through the edges. The observed patterns are in good agreement with the numerical solution of Eq. (1) using the boundary condition given by Eq. (2) and setting  $\eta = 0$  and  $H_a = 0$ . This boundary condition means that the tunneling current is fed into the junction through the edges, contrary to many other studies in which the bias current was assumed to be uniform. We believe this is a more appropriate model because it reduces to the well-known

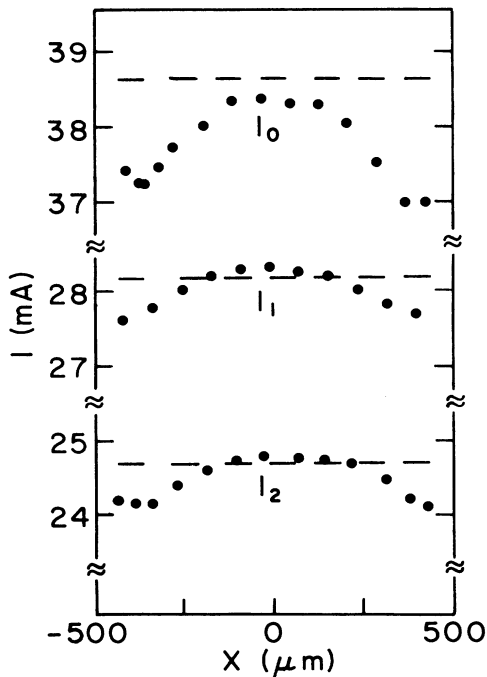


FIG. 1. The maximum zero-voltage current ( $I_0$ ) and the maximum dc currents of the first ( $I_1$ ) and the second ( $I_2$ ) zero-field steps as a function of the laser irradiation position  $x$ . The  $L/2\pi\lambda_J$  ratio is 3.

sine-Gordon equation and the boundary conditions which have been quite successful in describing the current distribution in the zero-voltage case.<sup>6,8</sup>

In Fig. 2 the simulated dynamic state with a soliton-antisoliton mode in the junction is shown in the left column. The solid curves show the phase-difference function  $\phi$ , its time derivative  $\dot{\phi}$ , and  $\sin\phi$  at  $t=0$ . Also included is the time-averaged spatially dependent  $\sin\phi$  to show the distribution of the pair current. The soliton in this case is represented by the  $2\pi$  kink in  $\phi$  near the center of the junction, and moves to the right. The dashed curves show the situations half a period later when the soliton has been reflected back as an antisoliton (antikink) and moves to the left. It is clear that the pair current associated with the soliton-antisoliton mode cancels. This means that the measured dc tunneling current is predominantly due to the zero-voltage current, that is, the current flowing in the region with zero voltage, even though the junction has a nonzero time-averaged voltage. The voltage pulse appears only where the traveling soliton or antisoliton is. We want to point out that the time-averaged pair-current distribu-

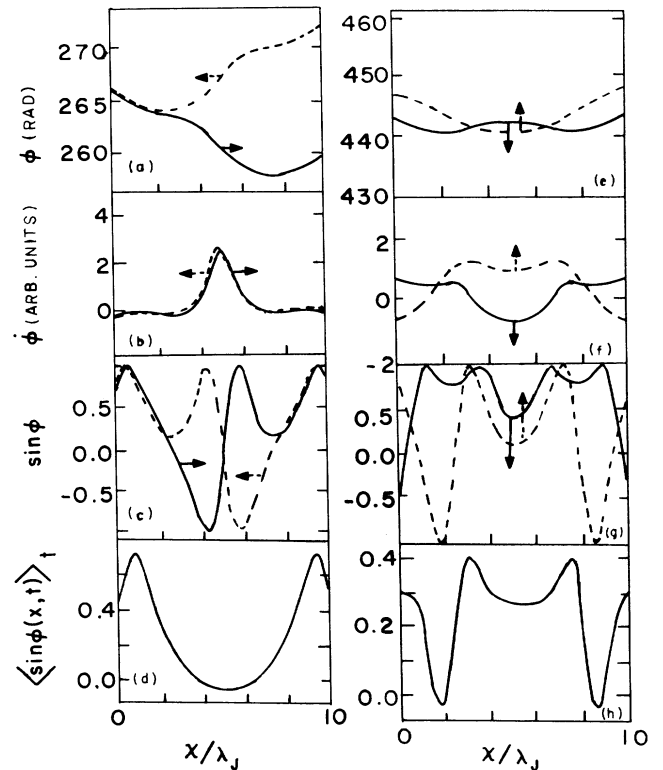


FIG. 2. The numerical results of the phase-difference function  $\phi(x,t)$ , its time derivative  $\dot{\phi}(x,t)$  representing the voltage, the normalized pair-current density  $\sin\phi(x,t)$ , and the time-averaged pair-current distribution  $\langle\sin\phi(x,t)\rangle_t$ . The dynamic state with a soliton-antisoliton mode propagating in the junction is shown in the left column. The right column shows the dynamic state associated with resonant symmetric mode. The dashed curves represent the situation at the time half a period after that of the solid curves. The arrows indicate the directions of movement.

tion is significant only near the edges similar to that of the static case.

Based on the information in Fig. 2, it is not difficult to understand the change in  $I_1$  and  $I_2$  shown in Fig. 1. Since the dc pair current is dominantly flowing near the edges, the instability of the soliton-antisoliton propagation occurs there. The focused laser irradiated at the junction edges effectively reduces the superconductivity there and makes the maximum current smaller. On the other hand, when the laser is focused at an area inside the junction, its only effect is to slow down the soliton-antisoliton mode somewhat by increasing the loss in that region. This reduction in the speed of soliton-antisoliton mode leads to a weaker impact with the junction edges. Consequently, the instability occurs at a slightly larger current. Furthermore, since the dc current is mainly the zero-voltage current near the edges, it does not depend on the number of solitons or antisolitons.

Also shown in the right-hand column of Fig. 2 is the dynamic state associated with the standing-wave excitation. We notice that all quantities have spatially oscillatory structures, including the dc pair-current density. As shown in Fig. 3, similar patterns have been observed in the changes in  $I_0$  and  $I_1$  with laser irradiation when an intermediate length junction was used.

The junction has a ratio of  $L/2\pi\lambda_J=1.2$  and can be classified as an intermediate junction. Figure 3(a) shows again that the zero-voltage current is concentrated near the edges similar to that shown in Fig. 1(a). However, the maximum current for the first step ( $I_1$ ) versus the laser position is distinctly different from that of Fig. 1(b). These results clearly demonstrate the difference in the two dynamic modes involved.

In conclusion, we have found that the zero-field current step of a one-dimensional Josephson junction can be associated with two different dynamic modes. The step arising from the soliton-antisoliton mode is largely the pair current flowing near the edges. On the other hand, the step due to standing waves has an oscillatory spatial distri-

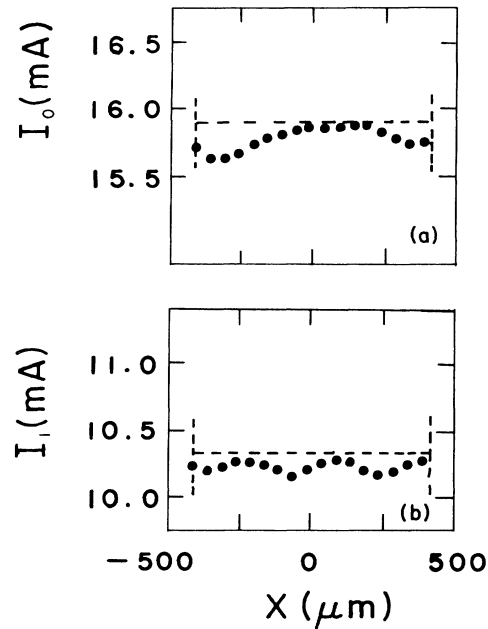


FIG. 3.  $I_0$  and  $I_1$  as a function of the laser irradiation position of a medium length junction with  $L/2\pi\lambda_J=1.2$ .

bution. According to the experimental results, the model in which the biased current is assumed to be near the junction edges seems to be more appropriate than those based on uniform bias current. We have also investigated the magnetic field dependence of the step heights in the presence of a laser beam both experimentally and theoretically. They are in good agreement and will be reported elsewhere.

This work was supported in parts by the National Science Foundation and the Institute for Manufacturing Research at Wayne State University.

- <sup>1</sup>B. D. Josephson, in *Superconductivity*, edited by R. D. Parks (Dekker, New York, 1969), Chap. 9, where an equation with  $\eta=0$  was derived; D. W. McLaughlin and A. C. Scott, *Phys. Rev. A* **18**, 1652 (1978), where an equation with a constant  $\gamma$  representing a uniform distribution of the bias current was discussed.
- <sup>2</sup>T. A. Fulton and R. C. Dynes, *Solid State Commun.* **12**, 57 (1973).
- <sup>3</sup>T. V. Rajeevakumar, J. X. Przybysz, J. T. Chen, and D. N. Langenberg, *Phys. Rev. B* **21**, 5432 (1980).
- <sup>4</sup>J. T. Chen, T. F. Finnegan, and D. N. Langenberg, *Physica* **55**, 413 (1971); J. T. Chen and D. N. Langenberg, in *Low Temperature Physics, LT-13, Proceedings of the Thirteenth International Conference*, edited by W. J. Sullivan and K. D. Timmerhaus (Plenum, New York, 1973), Vol. 3.
- <sup>5</sup>K. Takanaka, *Solid State Commun.* **29**, 443 (1979); Y. S. Gou and C. S. Chung, *J. Low Temp. Phys.* **37**, 367 (1979); Jhy-

- Jiun Chang, J. T. Chen, M. R. Scheuermann, and D. J. Scalapino, *Phys. Rev. B* **31**, 1658 (1985); H. Kawamoto, *Prog. Theor. Phys.* **66**, 780 (1981); **70**, 1171 (1983); Jhy-Jiun Chang and Y. W. Kim (unpublished).
- <sup>6</sup>M. R. Scheuermann, J. R. Lhota, P. K. Kuo, and J. T. Chen, *Phys. Rev. Lett.* **50**, 74 (1983); *Appl. Phys. Lett.* **44**, 255 (1984); Jhy-Jiun Chang, Ching-Hung Ho, and D. J. Scalapino, *Phys. Rev. B* **31**, 5826 (1985).
- <sup>7</sup>See also, S. C. Meepagala, W. D. Shen, P. K. Kuo, and J. T. Chen, in *Low Temperature Physics*, edited by U. Eckern, A. Schmid, W. Weber, and H. Wudl (Elsevier, Amsterdam, 1984), Vol. 17, pp. 473 and 474; Jhy-Jiun Chang, *Appl. Phys. Lett.* **47**, 431 (1985).
- <sup>8</sup>Jhy-Jiun Chang and D. J. Scalapino, *Phys. Rev. B* **29**, 2843 (1984); Jhy-Jiun Chang and C. H. Ho, *Appl. Phys. Lett.* **45**, 182 (1984); J. Bosch, R. Gross, M. Koyanagi, and R. P. Huebener, *Phys. Rev. Lett.* **54**, 1448 (1985).